Online MTPA Tracking for Optimal Performance of IPMSM based Compressor Drives

Visweshwar Chandrasekaran[1], *Member, IEEE*, Bernard Jose[2], *Member, IEEE,*
Ned Mohan[*], *Life Fellow, IEEE, Kaushik Basu[$], Senior Member, IEEE*
Email: viswesh@umn.edu, bernard.jose@tranetechnologies.com, mohan@umn.edu, kbasu@iisc.ac.in
[1]Trane Technologies, St. Paul, MN, USA, [2]Trane Technologies, Bangalore, India
[*]Department of Electrical and Computer Engineering, University of Minnesota, Minneapolis, MN, USA
[$]Division of EECS, Indian Institute of Sciences, Bangalore, India

***Abstract*— The efficiency of interior permanent magnet synchronous motors (IPMSM) can be directly influenced by Variable Frequency Drives (VFDs) implementing Maximum Torque Per Ampere (MTPA) algorithms. Model based optimization requires advanced knowledge of machine including non-linear properties which are quite pronounced in IPMSMs. This paper presents a novel online MTPA trajectory seeking scheme which is based on calculating the minimum current possible for every load operating point by dynamically adjusting the current angle during steady state operation. First, an offline MTPA trajectory is derived for the motor using simple datasheet parameters to get a baseline. Second, an online MTPA based on discrete extremum seeking state logic implemented using a model-based design approach is used to seek the least current for a given operating point. Key considerations have been made for efficient execution while minimizing computational resource requirements Experimental results obtained on a 3 *HP* IPMSM motor demonstrate the effectiveness of the proposed scheme in achieving the MTPA control objective while maintaining control stability across all operating regions.**

***Keywords*— maximum-torque-per-ampere (MTPA), interior permanent magnet machine (IPM), motor drive, variable frequency drive (VFD), inverter efficiency, field-oriented control (FOC), extremum seeking.**

I. INTRODUCTION

Power Electronic equipment such as Variable Frequency Drives (VFDs) are seeing increased usage in motor applications. This is due to the increased efficiency achieved by VFDs and the ability to precisely control factors such as speed and torque for the entire operation map of the equipment. IPMSMs have also gained significant popularity over the last several decades due to several advantages that include high power density and absence of significant rotor losses. However, the rotor construction in an IPMSM while taking advantage of dual torque mechanisms results in high magnetic saliency. This is reflected in non-equal quantities for the DQ axis inductances. Several research works take advantage of this phenomenon to extend and even optimize the machine design to efficiently operate under extended speed and torque range [2][3].

A popular scheme for IPMSM machines is MTPA which aims to deliver maximum efficiency across wide range of operation. A broad classification of various MTPA schemes and a comprehensive review of the advantages and disadvantages of the various schemes is summarized in a recently published survey article [1]. Initial research focused on maximizing efficiency for entire speed range [5][6]. It is most typical to formulate MTPA schemes based on predetermined tuning coefficients in combination with active and adaptive estimation and tracking [7][8]. Online MTPA schemes employ either minimum current search, signal injection or model-based techniques [9][10]. The performance of any MTPA scheme is dependent on accurate knowledge of motor parameters. The non-linear parameters of an IPMSM include (but not limited to) – stator resistance and magnet flux linkage (both of which vary with motor temperature) [11] and the $d-$ and $q-axis$ flux linkages (and hence inductances) which vary with $d-$ and $q-axis$ currents at a given operating point [12]. While online methods aim to achieve parameter insensitive execution, the implementation can be quite complex especially in cost sensitive applications and many methods still rely on Look Up Tables (LUTs) [13]. Several offline methods have been proposed which generate LUTs which may require large amount of memory and accurate interpolation algorithms [15].

The authors in [1] comment on the suitability of either the offline or the online method based on the requirements of the VFD development which may include factors such as – availability and confidence in machine parameters, desired dynamic response for the application, sensor robustness and accuracy, development and qualification time afforded to the technical team etc. A pragmatic approach to balancing the above-mentioned variables may be to develop a workflow that borrows the best practices of both the offline and online methods to create a hybrid solution. The authors of this paper previously published an efficient offline MTPA method that develops a 1D lookup function for the current angle and net current as a function of electromagnetic torque [16]. To develop the offline calculation of MTPA, 2D LUTs of the $d-$ and $q-axis$ flux linkages are obtained via Finite Element Modelling of the IPMSM machine. On a practical note, the competency of FEA modelling of machines is not readily available in many industries outside of motor and drive manufacturers.

In this paper, a cost and memory optimized online MTPA scheme is proposed with a discrete extremum seeking state

logic controller. To start with an offline method is employed to generate 1D functions of current and current angle using basic datasheet parameters. These functions are then improved in real-time with a novel perturb & observe scheme by manipulating the current angle which seeks the least possible operating current during steady state machine operation. The search algorithm for determining minimum current for every operating torque point is discussed, and experimental study has been carried out on a motor drive system to verify MTPA control performance.

II. Conventional MTPA Theory

The IPMSM is modelled in the synchronous DQ frame and is given by (1-2). For this study, a commercially available IPMSM has been selected. A destructive teardown of this motor sample provided knowledge of the machine's geometries and construction. The rotor consists of 2 pole pair interior buried magnets, as shown in Fig. 1, with bending flux paths along with a squirrel cage arrangement to help with line-starting the motor.

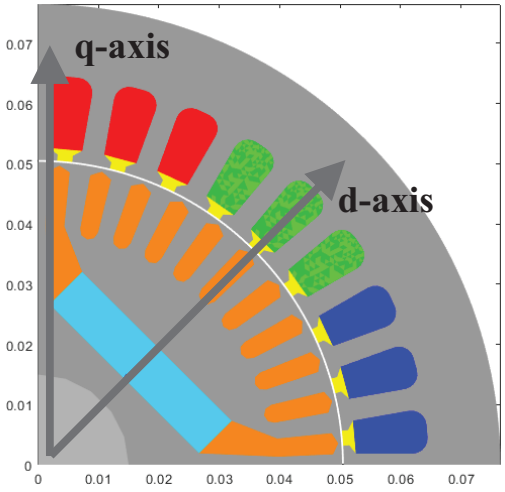

Fig. 1. Four Pole IPMSM geometry showing rotor magnet profile including rotor bars to aid in line-starting the machine

Due to the saliency in the rotor resulting from magnet placement, the flux distribution between the $d-$ and $q-$ axis are unique and are seen in the flux linkages λ_{ds} and λ_{qs}. It is well established in literature [3][19] that IPMSM have both self and cross saturation effects which result in 2D flux linkage or inductance maps that can be obtained either experimentally or via Finite Element Analysis (FEA) having knowledge of the machine geometry. These maps are shown in Fig. 3 and are given by (3-4).

Fig. 2 describes the voltage and current relationships in the DQ frame. The current angle, γ is defined as the angle between the $q-$axis current, I_{qs} and the net space vector current, I_{qds} of the machine at any given operating point. The work in this paper proposes a novel scheme to identify the optimal current angle and the corresponding least possible space vector current for every load operating point of the given IPMSM.

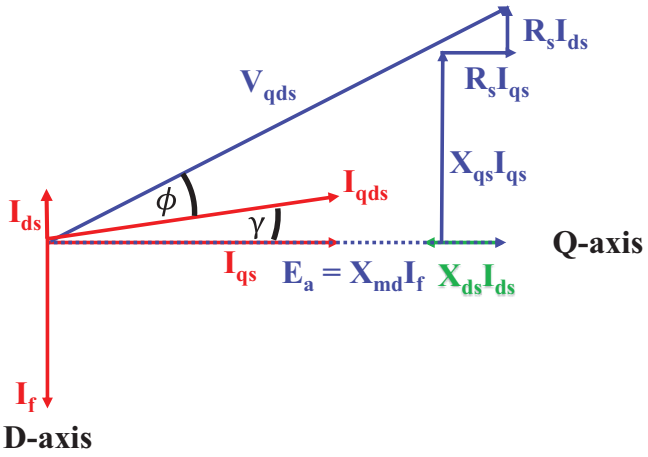

Fig. 2. Vector diagram of IPMSM voltage and current relationships

$$V_{qs} = R_s I_{qs} + \frac{d\lambda_{qs}}{dt} + \omega_e \lambda_{ds} \quad (1)$$

$$V_{ds} = R_s I_{ds} + \frac{d\lambda_{ds}}{dt} - \omega_e \lambda_{qs} \quad (2)$$

Where,

$$\lambda_d = L_{dd}(I_{ds}, I_{qs}) I_{ds} + L_{dq}(I_{ds}, I_{qs}) I_{qs} \quad (3)$$

$$\lambda_q = L_{qd}(I_{ds}, I_{qs}) I_{ds} + L_{qq}(I_{ds}, I_{qs}) I_{qs} \quad (4)$$

For an IPMSM the $d-$ and $q-axis$ inductances are not equal to each other which results in two torque mechanisms – magnet flux and reluctance torque given by (5) and further expressed in terms of DQ flux and currents as seen in (6)

$$T_{em} = T_{mag} + T_{rel} \quad (5)$$

$$T_{em} = \frac{3}{2}\frac{P}{2}\left(\lambda_d I_{qs} - \lambda_q I_{ds}\right) \quad (6)$$

In the conventional MTPA formulation, a simplifying assumption is often made to fix a single value of DQ inductance to derive the torque and current angle expressions. For a fixed value of inductance and ignoring machine saturation, (1) and (2) can be simplified to (7) and (8) respectively while (6) can be expanded in terms of DQ currents and Inductances as seen in (9).

$$V_{qs} = R_s I_{qs} + L_q \frac{dI_{qs}}{dt} + \omega_e L_d I_{ds} + \omega_e \lambda_{pm} \quad (7)$$

$$V_{ds} = R_s I_{ds} + L_d \frac{dI_{ds}}{dt} - \omega_e L_q I_{qs} \quad (8)$$

$$T_{em} = \frac{3}{2}\frac{P}{2}\left[\!\left[\lambda_m I_{qs} + \left(L_d - L_q\right) I_{qs} I_{ds}\right]\!\right] \quad (9)$$

From (8) it can be observed that when I_{ds} is fixed to a constant value (often simplified to $I_{ds} = 0$ for low-performance drives), the electromagnetic torque can be easily controlled by manipulating the I_{qs} quantity [19].

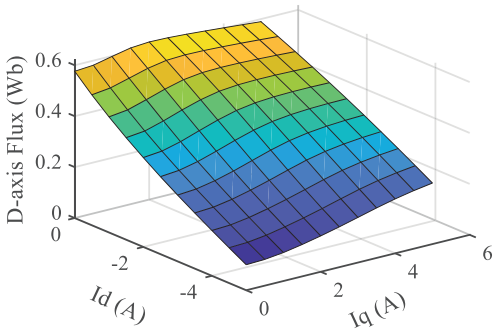

(a)

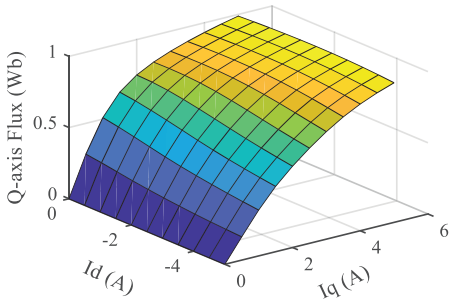

(b)

Fig. 3. 2D flux maps for (a) d −axis and (b) q −axis generated via FEA simulations

However, this simplification does not fully utilize the reluctance principle present in the IPMSM which is best utilized when I_{ds} is a dynamic non-zero quantity, changing with the operating point. This will result in a complex solution for determining the best combination of (I_{ds}, I_{qs}) to achieve the desired torque at the operating condition. The maximum output torque of an IPMSM is decided by the current and voltage limits which are represented by (10) and (11). The current limit circle is visualized in Fig. 5 for the motor being studied in this paper.

$$\sqrt{I_{ds}^2 + I_{qs}^2} \leq I_{qds} \tag{10}$$

$$\sqrt{V_{ds}^2 + V_{qs}^2} \leq V_{qds} \tag{11}$$

For a given torque demand at an operating point, line current amplitude is minimized to achieve the maximum torque. By placing the constraint of (9), the expression in (8) can be re-written to express torque as a function of I_{ds} and is given by (12)

$$T_{em} = \frac{3}{2}\frac{P}{2}\left[\lambda_m * \sqrt{(I_{qds})^2 - (I_{ds})^2} + I_{ds}(L_d - L_q)\sqrt{(I_{qds})^2 - (I_{ds})^2}\right] \tag{12}$$

Now, for the MTPA objective, a derivative of the above expression w.r.t I_{ds} can be written and solved $(\frac{dT_{em}}{dI_{ds}} = 0)$ to find the minimum solution of current to achieve demanded torque. This gives an expression for I_{qds} given by (13)

$$I_{qds} = \sqrt{2I_{ds}^2 + \frac{\lambda_m I_{ds}}{(L_d - L_q)}} \tag{13}$$

This expression for I_{qds} can then be substituted into (12) and simplified to yeild the below expression for torque as a function of d −axis current only as given by (14)

$$T_{em} = \frac{3}{2}\frac{P}{2}\left[\sqrt{I_{ds}^2 + \frac{\lambda_m I_{ds}}{(L_d - L_q)}}\right]\left[\lambda_m + (L_d - L_q)I_{ds}\right] \tag{14}$$

Using (14) and (9) a closed form solution can be obtained for $T_{em}(I_{ds}, I_{qs})$ for every operating point which satisfies the MTPA objective. For a simple model of the IPMSM ignoring flux/inductance saturation and keeping magnet flux linkage as constant, the MTPA trajectory follows the conventional line shown in Fig. 5.

An alternate solution for determining the optimal current angle for every operating point is well reported in literature [21][8][22] and is given by (15)

$$\gamma = sin^{-1}\left(\frac{-\lambda_m + \sqrt{\lambda_m^2 + 8(L_d - L_q)I_{qds}^2}}{4(L_d - L_q)I_{qds}}\right) \tag{15}$$

As mentioned previously, in considering the above analytical approaches to solve for MTPA condition, motor parameters such as L_d, L_q and λ_m are considered constant and independent of motor operating point. This implies that the effects of self- and cross-saturation are being ignored. However as can be seen in Fig. 4 L_d and L_q exhibit saturation effects with loading. The goal of this study is to examine and formulate an online MTPA trajectory while considering such non-linear properties of the IPMSM. Starting with an offline MTPA trajectory generated from simple unsaturated datasheet parameters, a perturb & observe state logic has been implemented which achieves "last mile" performance improvement. The non-linear property of PM flux linkage and hence back electro-motive force (BEMF) variation as a function of temperature is kept out of the scope of this paper as all experiments were conducted while keeping the motor sample at room temperature. Further reading on this subject can be found in [19] and [20].

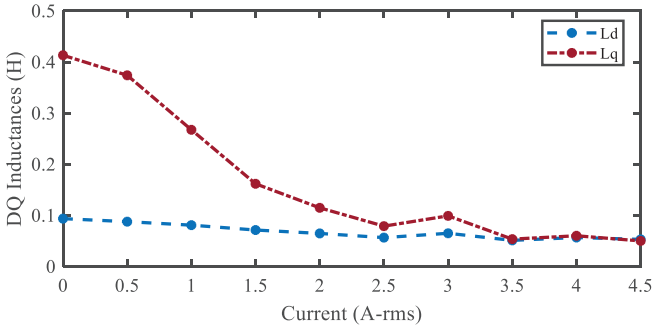

Fig. 4. Profile of d − and q −axis inductances showing non-linear saturation

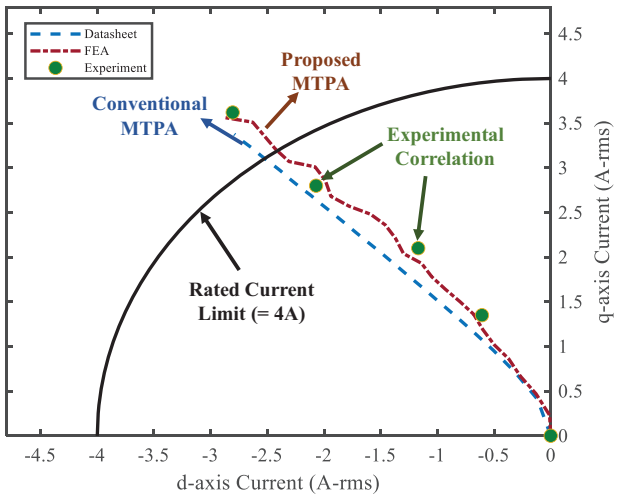

Fig. 5. MTPA trajectories showing results of simple datasheet parameters and that of non-linear parameters obtained via FEA. Experimental testpoints using proposed method match FEA trajectory within reasonable error

III. Proposed Model Based Online MTPA Scheme

As a case study, Fig. 6 captures the multiple solutions of current, I_{qds}, to achieve the demand torque. This data is solved for the various combinations of $L_d(I_{ds}, I_{qs})$ and $L_q(I_{ds}, I_{qs})$ sourced from FEA data shown in Fig. 3. The optimal solution lies along the trajectory highlighted in dashed red while the other operating points may still generate torque albeit with poorer efficiency.

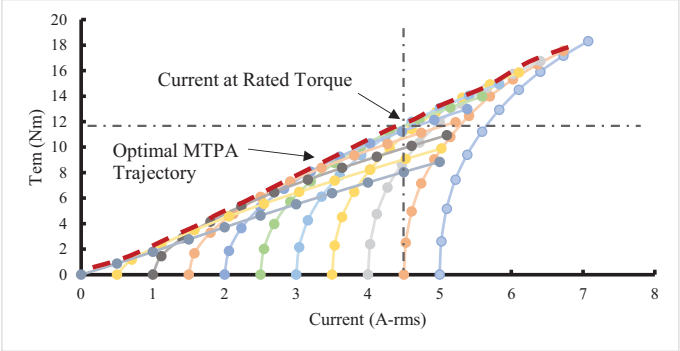

Fig. 6. Graph showing multiple solutions for stator currents for every operating point and MTPA trajectory optimizing current for each torque r

The MTPA tracking technique proposed in this paper is based on identifying the minimum possible operating space vector current, I_{qds} at a given steady state condition. The proposed method develops on the foundational work described in [16]. Two cascaded calculation loops are developed – outer torque and inner current angle. By fixing a range of current angles $[0{:}\gamma_{max}]$, it is possible to scan through each operating condition of torque and solve for all values of γ and I_{qds} using (14). At the next iteration, the torque reference is incremented by a certain factor and a new minimum result is computed using the same procedure considering the range of γ. The deviation from [16] is to utilize simple datasheet values of L_d and L_q in (14) as opposed to FEA based saturated parameters used in this previous work. This modification eliminates the requirement of needing FEA analysis to develop the MTPA scheme. The resultant optimal values of space vector current, I_{qds} and current angle, γ are stored into 1D LUTs. This procedure happens once during the commissioning of a VFD with a new motor application. The 1D LUTs are visualized in Fig. 11 as the dotted blue lines. These curves are to be treated as a non-efficient MTPA trajectory which will be further improved via the proposed online method. This will lead the operating curves to follow the FEA generated trajectory shown by dotted red lines also in Fig. 11. It is to be noted that the authors chose to use the terminology of "Model Based Design" to communicate the method of developing the state logic controls using graphical tools such as MATLAB/Simulink. Another interpretation of model-based design in literature is when methods make use of physical modelling of the IPMSM as a basis for the algorithm [24].

Using the offline scheme developed in [16] the plots of minimum currents are shown in Fig. 7. A deviation in current angle is seen between a simple datasheet-based solution and FEA parameter-based method. Two observations can be made from the plots. Firstly, the solution curve using FEA is flatter across the load range when compared to simple datasheet. This indicates the solution for minimum current can be attained with a wider range of current angles. Secondly, the deviation in the two solutions (shown as shaded gray areas in the plot) show a pattern where the FEA method solves for a lower current for lighter loads (compared to datasheet) and moves towards higher relative currents at higher loads. Both observations can be explained by the saturating and coupled nature of the flux linkages which are more pronounced at higher load. This information is missing in the simple datasheet and becomes the goal of the seeking logic in the proposed online method.

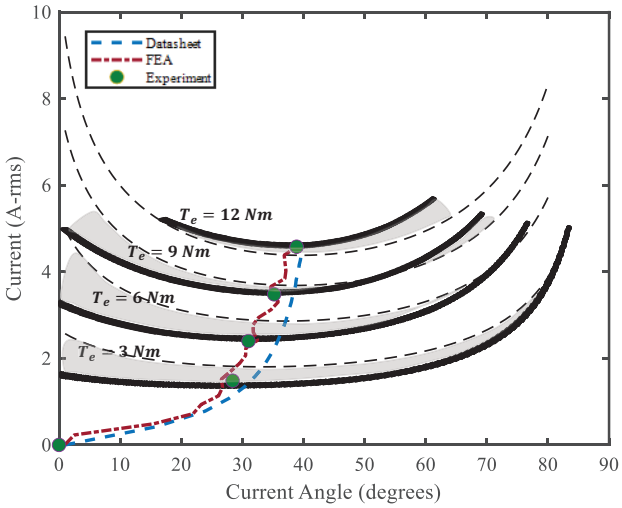

Fig. 7. Minimum current solution and corresponding current angle for each iteration of torque are shown for the offline method that uses simple datasheet (dotted lines) or saturated flux tables from FEA (bold lines). Experimental results using proposed method have close correlation to FEA based trajectory

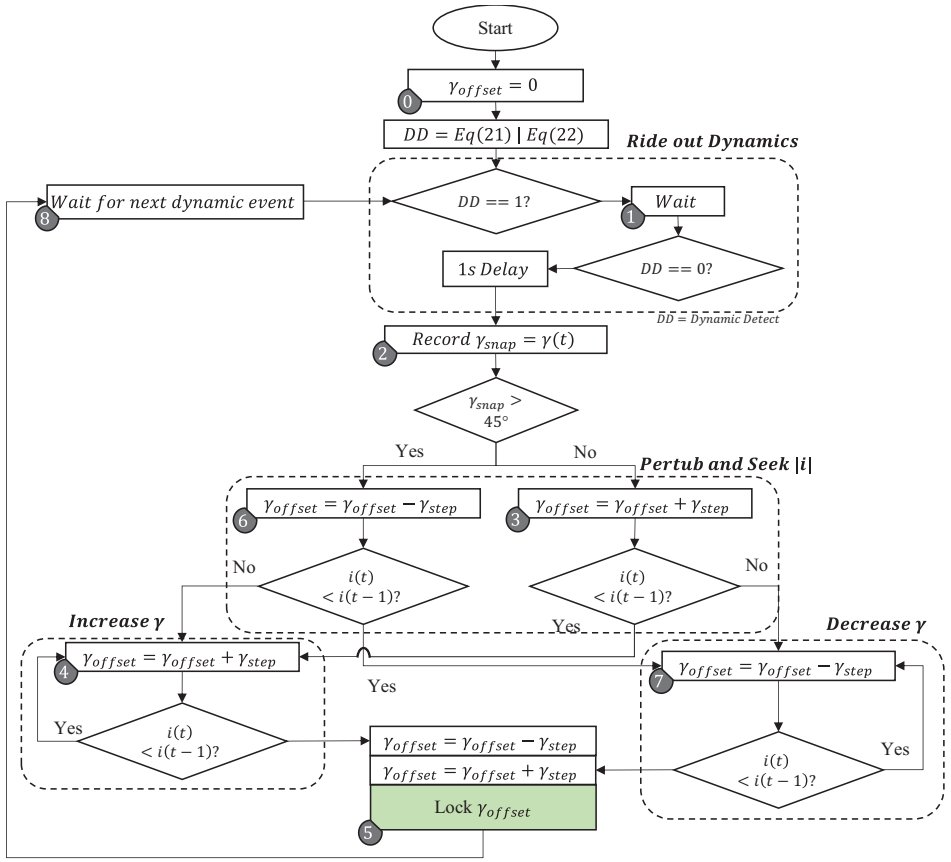

Fig. 8. Proposed MTPA scheme using extermum seeking state logic

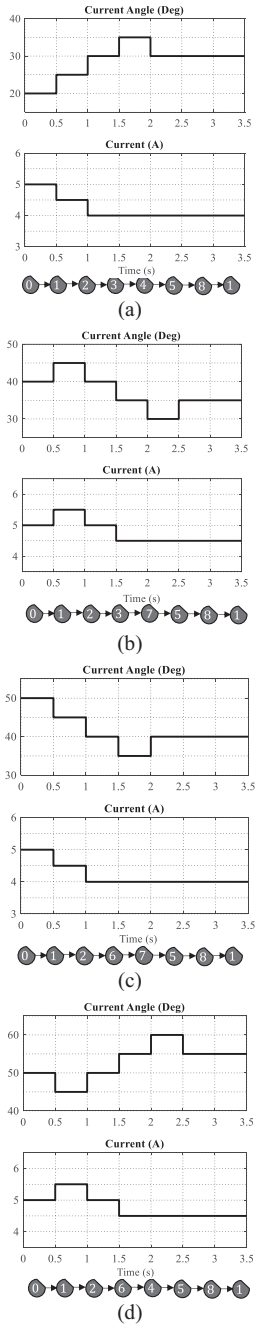

Fig. 9. Timing plots showing the perturb & observe logic with four scenarios of current response with change in current angle

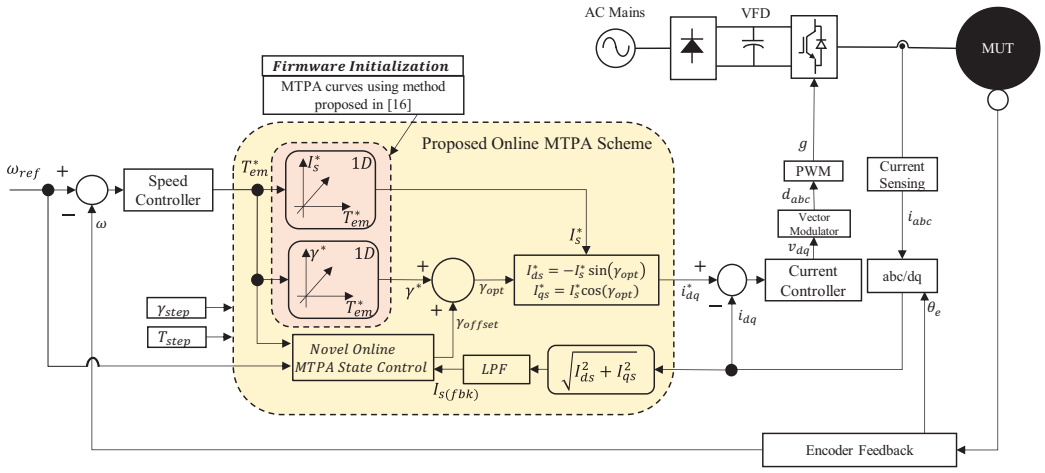

Fig. 10. Conventional Field Oriented Control (FOC) of IPMSM using the proposed online MTPA method

Fig. 8 shows the state logic for the proposed MTPA scheme that is inserted between the speed and current regulators in a conventional FOC control scheme. The method is constrained to operate only during steady state machine operation. Hence a simple "dynamic detect" logic is implemented where the current value of actual motor speed and estimated torque are compared with previous instance. A logic bit – DD – asserts when the difference is within a user defined range. This is expressed in (21) and (22) and once asserted activates the perturb & observe logic.

$$|\omega_m(t-1) - \omega_m(t)| > x\% * \omega_{m(rated)} \quad (21)$$

$$|T^*_{em}(t-1) - T^*_{em}(t)| > y\% * T_{em(rated)} \quad (22)$$

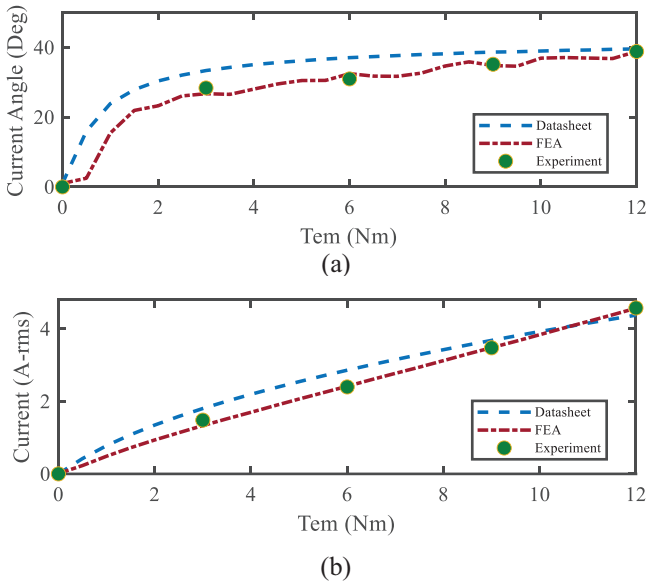

Fig. 11. Current angle (a) and RMS current (b) relationship with torque for zero to rated condition are shown for all three methods M1-M3 along with test datapoints

Once the state controller detects steady state conditions, a snapshot of the current operating current angle is recorded. The current angle, γ is typically in the range of $0-90°$ and $45°$ is the flip over point for dominant utilization of $d-$axis current. Based on the present value of γ a step change in the angle is introduced either in the positive or negative direction and the measured current magnitude change is observed. With a goal of minimizing current, γ could follow one of the four proposed paths shown in Fig. 9. Once a current minimum is found and no further improvement is seen, the angle offset, γ_{offset} is locked for the operating point. The logic goes into a standby state waiting for the next dynamic load change event to repeat the optimum angle search sequence. Fig. 10 shows the implementation of the proposed MTPA state controller in the FOC architecture. The implementation is targeted for applications with slow torque dynamics and regulated speed control such as fan and compressor drives. Hence the perturbation timing is intentionally elongated to avoid torque or speed oscillations. Tuning parameters such as γ_{step} and T_{step} can be adjusted to control the offset angle step and time respectively which can increase speed and performance of the algorithm.

IV. Simulation Results

Simulations have been performed on a 3 HP IPMSM whose vendor provided datasheet is listed in Table I. Fig. 12(c) shows the application of current angle steps to seek the minimum current. The plots are visualized after motor reached steady state speed and torque tracking 1500 RPM and 6.7 Nm respectively. The current angle steps are applied at $0.5s$ intervals with $\gamma_{step} = 5°$ increments. The response follows the state transition scenario shown in Fig. 9(c). The proposed algorithm results in a 6.15% improvement in net current at this operating point. During the γ_{step} application, the speed regulation occurs without any noticeable instability as does the electromagnetic torque delivery of the motor to maintain load.

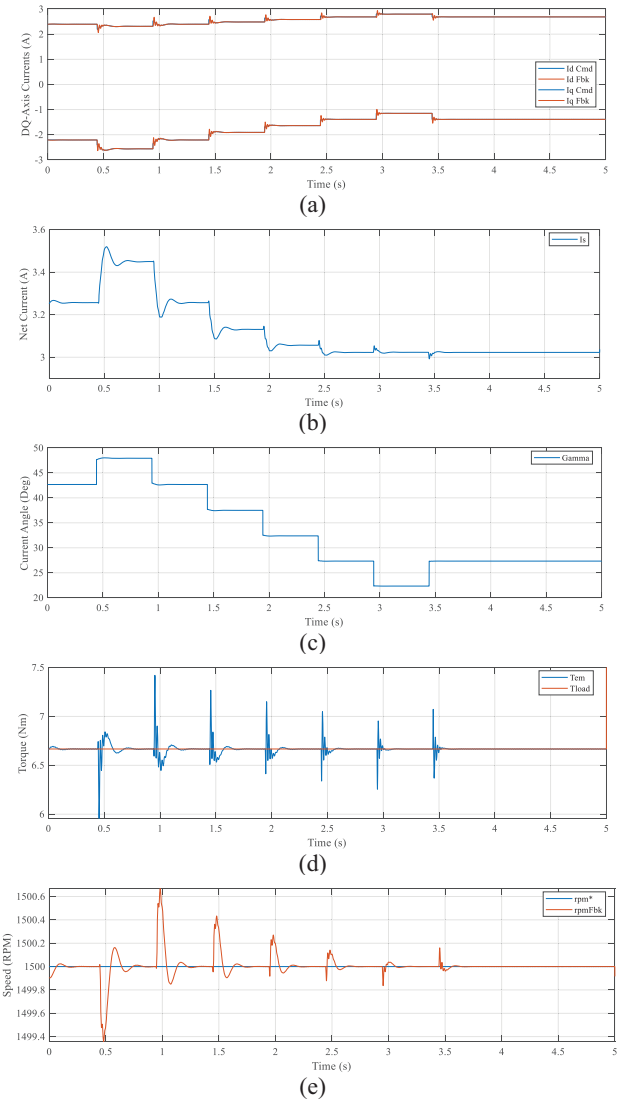

Fig. 12. Simulation results showing $d-$axis and $q-$axis current tracking in (a) and (b), Current Space Vector in (c), Current Angle calculated via proposed MTPA algorithm in (d), Electromagnetic Torque estimated via controller a and load torque measured in (e) and 3 phase motor currents zoomed into a steady state region in (f)

V. Experimental Validation

In this section, experimental results are presented to demonstrate the accuracy of the MTPA trajectory obtained via the proposed model based offline scheme. A state machine first starts the controller into "initialization" state which enables the offline MTPA trajectory calculation and the resulting LUT arrays for space vector current, $I_{qds(MTPA)}$ and current angle γ_{MTPA} are stored in memory. The state machine then goes to "active" state which starts the motor control scheme. The MTPA LUTs are utilized by the proposed online scheme to further fine tune the non-optimal control towards seeking the efficient control performance. The proposed model based MTPA scheme as well as the FOC control

algorithm has been developed in MATLAB/Simulink and auto-code generation tools have been used to generate the code. The code has been deployed on a Performance Real-Time target from Speedgoat. The Speedgoat controller consists of a 4.2 GHz Quad core Intel i7 CPU operating with Simulink Real Time operating system. The peripherals such as Analog, Digital I/O's as well as PWM are implemented on a Xilinx Kintex-7 FPGA option card called IO334 with a based clock rate of $10ns$. While this controller significantly exceeds the requirements of the proposed control scheme, the authors have taken advantage of the rapid prototyping capabilities offered by Speedgoat.

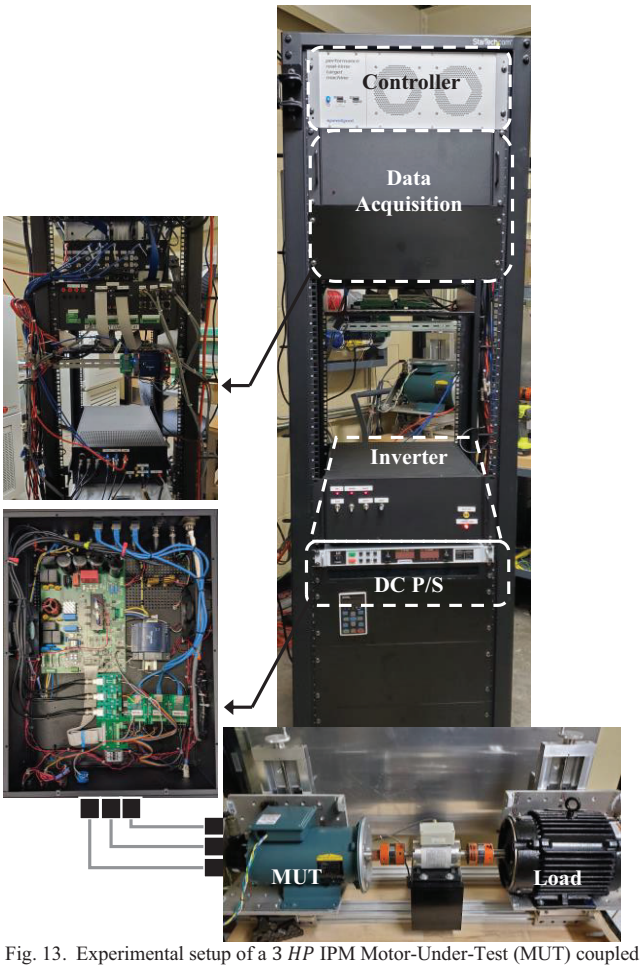

Fig. 13. Experimental setup of a 3 HP IPM Motor-Under-Test (MUT) coupled to a matched 3 HP PM based load motor. MUT driven via classic 2-L VSI DC-fed Inverter

A power inverter has been developed based on the classic 2-Level (2L) Voltage Source Inverter (VSI) topology. An evaluation board with P/N: EVAL-M5-IMZ120R-SIC has been sourced from Infineon Technologies for the power inverter. A custom data acquisition system has also been developed to measure various feedback quantities such as quadrature encoder, shaft torque, motor voltages and currents. The MUT used in this study is a 3 HP IPMSM from Baldor with P/N: CSPM3611T while the load motor is a 3 HP IPMSM from Marathon with P/N SY006A. The vendor provided datasheet is shown in Table I.

TABLE I. IPMSM Parameters from Vendor Datasheet

Parameter	Value
Rated Power	3 HP
Rated Voltage	460 $V-rms$
Rated Speed	1800 r/min
Rated Current	4 $A-rms$
Rated Torque	12 Nm
Stator Resistance, R_s	2.184 Ω
Direct Axis Inductance, L_d	10.393 mH
Quadrature Axis Inductance, L_q	300 mH
Magnet Flux Linkage, λ_{pm}	0.376 Wb
No. of Poles, P	4
Inertia, J	0.011 $kg.m^2$

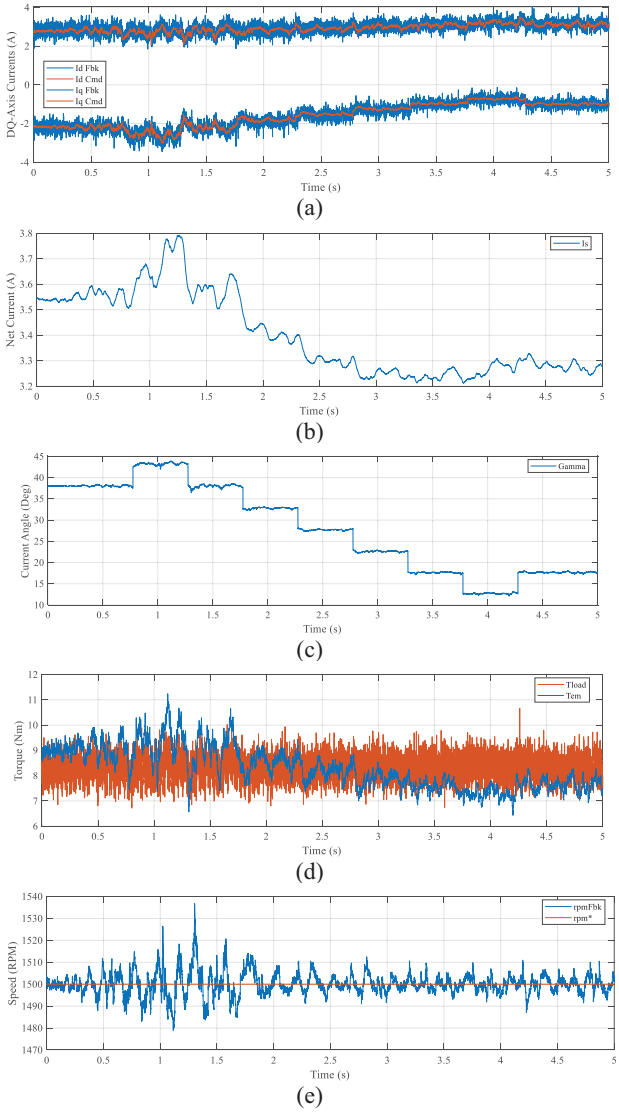

Fig. 14. Experimental results showing $d-$axis and $q-$axis current tracking in (a), Current Space Vector in (b), Current Angle calculated via proposed MTPA algorithm in (c), Electromagnetic Torque estimated via controller a and load torque measured in (d) and measured motor speed tracking setpoint in €

The control scheme is implemented with the outer speed regulator running at $5\,Hz$ bandwidth while the inner current regulator is running at $100\,Hz$. The inverter switching frequency is programmed at $4\,kHz$ which represents a typical configuration for most industrial drives across multiple industries. The details of the controller design are beyond the scope of this paper and can be found in [17].

Plots in Fig. 14 show the experimental results for a similar operating point as seen in simulation. The MUT is operated at $1500\,r/min$ with a steady load of ~75%. Fig 14(b) and (c) show the application of current angle steps and corresponding current response. A reduction in net current is seen at the completion of the state logic showing a 8.45% improvement at this operating point. It is to be noted that there will be practical differences between the electromagnetic torque and mechanical output load torque owing to core losses in motor as well as mechanical losses in the shaft assembly. Characterizing these losses is beyond the scope of this paper and is detailed in [19]. Steady state points obtained via experiments are overlayed onto the proposed trajectory in Fig. 5, 7 and 11 which show the tracking error of the algorithm to be under 1%.

VI. Conclusions

The torque production of an IPMSM over its operating speed range has strong dependency on the allocation of net current between the $d-$ and $q-axis$ components. The MTPA condition is affected by the machine's parameters where flux saturation plays a significant role. The work in this study proposes an online extremum seeking scheme which considers inductance variation across operating map and calculates the optimal current angle, γ which helps achieve minimum current for the torque demand. This method works consistently across the speed range of the machine as the mechanical time constant does not impact the torque optimization objective except during dynamic speed change. The proposed algorithm is constructed with a focus on minimizing the computational demand thus enabling wider adaptation in cost sensitive applications. Simulation and experimental results show tight correlation with less than 1% error in optimized current for the given torque demand when compared to FEA generated data.

References

[1] Dianov, Anton, et al. "Review and classification of MTPA control algorithms for synchronous motors." IEEE Transactions on Power Electronics (2021).

[2] Morimoto, Shigeo, et al. "Expansion of operating limits for permanent magnet motor by current vector control considering inverter capacity." *IEEE transactions on industry applications* 26.5 (1990): 866-871.

[3] Bianchi, Nicola, and Thomas M. Jahns. "Design analysis and control of interior PM synchronous machines." *Tutorial Course Notes, IEEE-IAS* 4 (2004).

[4] Tinazzi, F., et al. "Classification and review of MTPA algorithms for synchronous reluctance and interior permanent magnet motor drives." *2019 21st European Conference on Power Electronics and Applications (EPE'19 ECCE Europe)*. IEEE, 2019.

[5] R. F. Schiferl and T. A. Lipo, "Power capability of salient pole permanent magnet synchronous motors in variable speed drive applications," IEEE Trans. Ind. Appl., vol. 26, no. 1, pp. 115–123, Jan 1990

[6] S. Morimoto, M. Sanada, and Y. Takeda, "Wide-speed operation of interior permanent magnet synchronous motors with high-performance current regulator," IEEE Trans. Ind. Appl., vol. 30, no. 4, pp. 920–926, July 1994

[7] Dianov, Anton, et al. "Robust self-tuning MTPA algorithm for IPMSM drives." *2008 34th Annual Conference of IEEE Industrial Electronics*. IEEE, 2008.

[8] Niazi, Peyman, Hamid A. Toliyat, and Abbas Goodarzi. "Robust maximum torque per ampere (MTPA) control of PM-assisted SynRM for traction applications." *IEEE transactions on vehicular technology* 56.4 (2007): 1538-1545.

[9] Windisch, Thomas, and Wilfried Hofmann. "A novel approach to MTPA tracking control of AC drives in vehicle propulsion systems." *IEEE Transactions on Vehicular Technology* 67.10 (2018): 9294-9302.

[10] Bolognani, S., L. Sgarbossa, and M. Zordan. "Self-tuning of MTPA current vector generation scheme in IPM synchronous motor drives." 2007 European Conference on Power Electronics and Applications. IEEE, 2007.

[11] S. Bolognani,R. Petrella, A. Prearo, and L. Sgarbossa, "Automatic tracking of MTPA trajectory in IPM motor drives based on ac current injection," IEEE Trans. Ind. Appl., vol. 47, no. 1, pp. 105–114, Jan. 2011.

[12] Sebastian, Tomy. "Temperature effects on torque production and efficiency of PM motors using NdFeB magnets." IEEE Transactions on Industry Applications 31.2 (1995): 353-357.

[13] Sneyers, Brigette, Donald W. Novotny, and Thomas A. Lipo. "Field weakening in buried permanent magnet ac motor drives." IEEE Transactions on Industry Applications 2 (1985): 398-407.

[14] Kim, Sungmin, et al. "Maximum torque per ampere (MTPA) control of an IPM machine based on signal injection considering inductance saturation." *IEEE Transactions on Power Electronics* 28.1 (2012): 488-497.

[15] Bae, Bon-Ho, et al. "New field weakening technique for high saliency interior permanent magnet motor." 38th IAS Annual Meeting on Conference Record of the Industry Applications Conference, 2003.. Vol. 2. IEEE, 2003.

[16] Chandrasekaran, Visweshwar, et al. "Offline Model Based MTPA Methodology for Optimum Performance of Interior Permanent Magnet Machines over Full Range of Speed and Torque", accepted for publication at *2021 IEEE Transportation Electrification Conference & Expo (ITEC)*. IEEE, 2021.

[17] Chandrasekaran, Visweshwar, et al. "A novel model based development of a motor emulator for rapid testing of electric drives." 2020 IEEE Energy Conversion Congress and Exposition (ECCE). IEEE, 2020.

[18] Xia, Zekun, et al. "Online optimal tracking method for interior permanent magnet machines with improved MTPA and MTPV in whole speed and torque ranges." *IEEE Transactions on Power Electronics* 35.9 (2020): 9753-9769.

[19] Pellegrino, Gianmario, et al. *The rediscovery of synchronous reluctance and ferrite permanent magnet motors: tutorial course notes*. Springer, 2016.

[20] Krishnan, R., and Praveen Vijayraghavan. "Fast estimation and compensation of rotor flux linkage in permanent magnet synchronous machines." *ISIE'99. Proceedings of the IEEE International Symposium on Industrial Electronics (Cat. No. 99TH8465)*. Vol. 2. IEEE, 1999.

[21] Morimoto, Shigeo, et al. "Expansion of operating limits for permanent magnet motor by current vector control considering inverter capacity." IEEE transactions on industry applications 26.5 (1990): 866-871.

[22] Morimoto, Shigeo, et al. "Servo drive system and control characteristics of salient pole permanent magnet synchronous motor." *IEEE Transactions on Industry Applications* 29.2 (1993): 338-343.

[23] T. Windisch and W. Hofmann, "A comparison of a signal-injection method and a discrete-search algorithm for MTPA tracking control of an IPM machine," 2015 17th European Conference on Power Electronics and Applications (EPE'15 ECCE-Europe), 2015, pp. 1-10, doi: 10.1109/EPE.2015.7309290.

[24] Windisch, Thomas, and Wilfried Hofmann. "A novel approach to MTPA tracking control of AC drives in vehicle propulsion systems." IEEE Transactions on Vehicular Technology 67.10 (2018): 9294-9302.